Current Biology *16*, 195–201, January 24, 2006 ©2006 Elsevier Ltd All rights reserved DOI 10.1016/j.cub.2005.12.011

Report

The Class I PITP Giotto Is Required for *Drosophila* Cytokinesis

Maria Grazia Giansanti,[1] Silvia Bonaccorsi,[1] Roman Kurek,[1] Rebecca M. Farkas,[2,3] Patrizio Dimitri,[1] Margaret T. Fuller,[2] and Maurizio Gatti[1,*]

[1] Dipartimento di Genetica e Biologia Molecolare
Istituto Pasteur-Fondazione Cenci Bolognetti
Istituto di Biologia e Patologia Molecolari del CNR
Università di Roma "La Sapienza"
P.le A. Moro 5
00185 Roma
Italy

[2] Department of Genetics

[3] Department of Developmental Biology
Stanford University School of Medicine
Stanford, California 94305

Summary

Phosphatidylinositol transfer proteins (PITPs) are highly conserved polypeptides that bind phosphatidylinositol or phosphatidylcholine monomers, facilitating their transfer from one membrane compartment to another [1]. Although PITPs have been implicated in a variety of cellular functions, including lipid-mediated signaling and membrane trafficking, the precise biological roles of most PITPs remain to be elucidated [1, 2]. Here we show for the first time that a class I PITP is involved in cytokinesis. We found that *giotto (gio)*, a *Drosophila* gene that encodes a class I PITP, serves an essential function required for both mitotic and meiotic cytokinesis. Neuroblasts and spermatocytes from *gio* mutants both assemble regular actomyosin rings. However, these rings fail to constrict to completion, leading to cytokinesis failures. Moreover, *gio* mutations cause an abnormal accumulation of Golgi-derived vesicles at the equator of spermatocyte telophases, suggesting that Gio is implicated in membrane-vesicle fusion. Consistent with these results, we found that Gio is enriched at the cleavage furrow, the ER, and the spindle envelope. We propose that Gio mediates transfer of lipid monomers from the ER to the equatorial membrane, causing a specific local enrichment in phosphatidylinositol. This change in membrane composition would ultimately facilitate vesicle fusion, allowing membrane addition to the furrow and/or targeted delivery of proteins required for cytokinesis.

Results and Discussion

The *gio* Complementation Group

We identified the first *gio* mutant allele, gio^{Z3934}, in the course of a screen for mutants defective in spermatocyte cytokinesis [3]. Flies homozygous for gio^{Z3934} show frequent multinucleate spermatids [3] (Figure 1C), a phenotype diagnostic of failures in meiotic cytokinesis [3, 4]. *gio* maps to the third chromosome and is uncovered by *Df(3R)D1-BX12* that removes the polytene chromosome interval 91F-92D6 [3]. Complementation tests with P element insertions mapping to the same interval showed that the P-induced lethals gio^{RM1}, gio^{j5A6}, and gio^{EP513} fail to complement each other and gio^{Z3934} for the defect in meiotic cytokinesis (Figures 1A and 1D). In addition, larval brains of these lethal mutants exhibit frequent polyploid cells but have normal frequencies of anaphases (Figures 1A and 2D), consistent with a defect in neuroblast cytokinesis [5].

gio Encodes a Class I PITP

gio^{RM1} is a P-induced mutation generated in our laboratory; inverse PCR and sequencing experiments revealed that the P element responsible for this mutation is inserted into the first, untranslated exon of the predicted *CG5269* gene (Figure 1B). Transposase-induced precise excision of this P element rescued all mutant phenotypes associated with gio^{RM1}. gio^{j5A6} is another P-induced mutation with the P element inserted within the first intron of the *CG5269* gene, while gio^{EP513} carries an EP element inserted very close to that of gio^{RM1} (FlyBase, http://flybase.bio.indiana.edu; Figure 1B). EP elements contain a GAL4 binding site and a weak promoter and have the ability to drive the directional expression of adjacent genes in the presence of GAL4 [6]. GAL4-driven expression of the *CG5269* gene rescued all the mutant phenotypes associated with the *gio* mutations (see Supplemental Experimental Procedures available with this article online). Together, these results indicate that *gio* corresponds to the *CG5269* gene. We also sequenced all the exons of the EMS-induced gio^{Z3934} mutant gene but did not find any mutation. This suggests that the gio^{Z3934} allele carries a mutation in the promoter region.

The *CG5269* gene encodes a 272 aa polypeptide of 35 kDa that is closely related to phosphatidylinositol (PtdIns) transfer proteins (PITPs). In animal cells, the PITPs comprise small soluble 32–35 kDa proteins containing a single PtdIns transfer domain (class I PITPs), as well as larger integral membrane proteins possessing additional domains (class II PITPs) [1, 2]. While in mammals there are five PITPs, *Drosophila* has only three proteins of this family [1, 2]. Class II PITPs include the *Drosophila* RdgB2 and Rdg2Bβ proteins and the three human polypeptides Nir1, Nir2, and Nir3. RdgB2 is encoded by the *retinal degeneration B (rdgB)* gene, which serves a nonessential function specifically required for phototransduction and prevention of retinal degeneration; the wild-type function of the *rdgBβ* gene is currently unknown [2]. Ablation of mouse *Nir2* results in early embryonic death, and its expression in *Drosophila* can rescue the mutant phenotypes elicited by *rdgB2* mutations. In addition, Nir2 is essential for completion of cytokinesis in human cells [2, 7]. The mouse Nir3

*Correspondence: maurizio.gatti@uniroma1.it

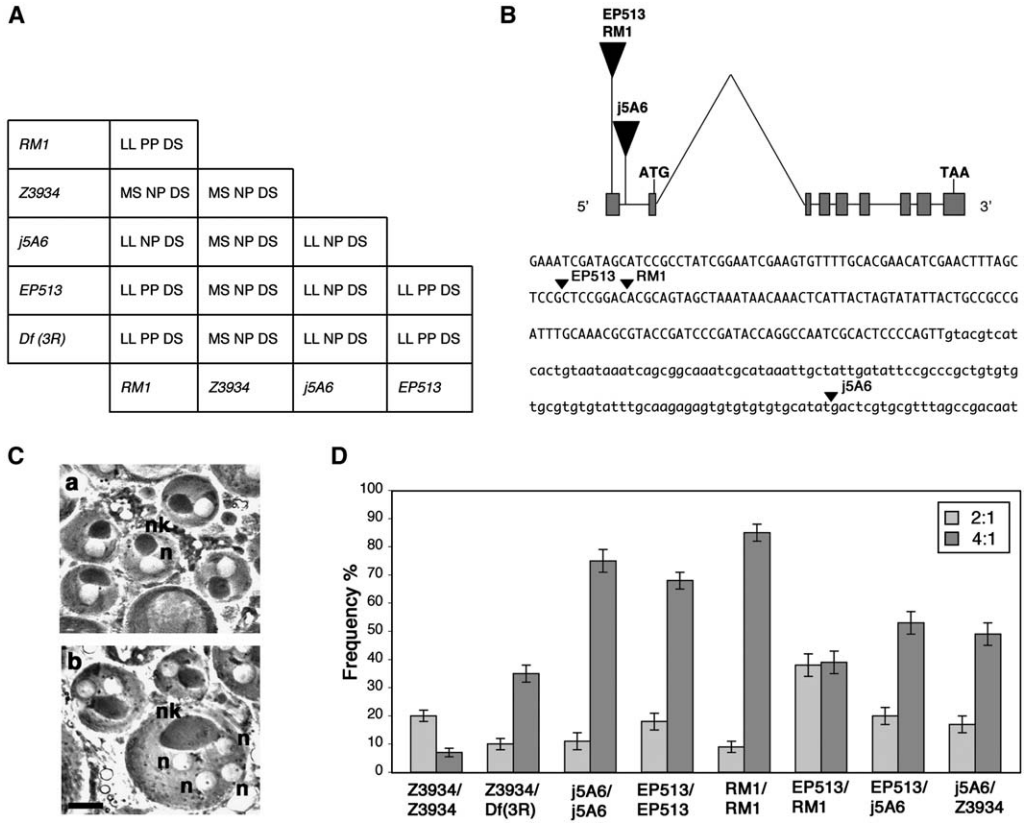

Figure 1. The *giotto* Complementation Group

(A) Complementation analysis among *gio* mutant alleles. LL, late lethal; MS, viable, male sterile; PP, polyploid cells in larval brains; NP, no polyploid cells in larval brains; DS, defective spermatids.

(B) Top: Map of the *gio* locus showing the exon/intron organization, the positions of the ATG and stop (TAA) codons, and the positions of P element insertions associated with the *gio* mutations used in this study (large inverted triangles). Bottom: Partial DNA sequence showing the precise localization of the P element insertions (small inverted triangles). Exon and intron sequences are in capital and lower case letters, respectively.

(C) Abnormal spermatids observed in living *gio* mutant testes. (a) Wild-type spermatids with nuclei (n, white circles) and nebenkern (nk, dark circles) of similar sizes. (b) Multinucleated spermatids from *gio* mutants containing two (2:1) or four (4:1) nuclei of similar sizes associated with a single large nebenkern. Scale bar equals 10 μm.

(D) Frequencies (± SE) of abnormal spermatids observed in *gio* mutant males. In wild-type males, the frequency of abnormal spermatids is virtually zero.

gene is not required for photoreceptor function or survival, and its function is currently unclear [1, 2].

Mammalian cells contain two class I PITPs, PITPα and PITPβ, that share 77% sequence identity. PITPβ deficiency in mouse results in early failure of embryonic development, whereas ablation of PITPα does not compromise embryonic stem cell viability but leads to severe neurodegenerative disorders, including the vibrator phenotype observed in hypomorphic mutations [1, 2, 8]. An alignment of the predicted Gio protein with its mammalian homologs revealed that Gio is 61%–62% and 59% identical to mammalian PITPβ and PITPα, respectively. In addition, phylogenetic analysis with the PHYLIP suite showed that Gio is closer to the β than to the α isoform. Thus, we propose to call the *CG5269* gene *giotto* instead of *vibrator* (see Supplemental Experimental Procedures).

Gio Is Required for Actomyosin Ring Constriction

Previous studies revealed that gio^{Z3934} spermatocytes are defective in contractile ring constriction and furrow ingression [3]. To confirm these results, we examined gio^{RM1} mutant testes stained for chromatin, tubulin, and F-actin. In gio^{RM1} males, early meiotic telophases were completely normal and displayed regular actin rings and central spindles (Figure S1). The central spindle and the contractile ring remained normal also in most mutant midtelophases. However, most late telophases from gio^{RM1} mutants displayed actin rings that were not fully constricted (Figures 2A, part b, and 2B). In addition, in 11% of these late telophases, the actin rings were either discontinuous or absent and the central spindles less dense than in wild-type (Figures 2A, part c, and 2B).

We next determined the cytokinesis phenotype of *gio* mutant neuroblasts (NBs) by examining brain preparations stained for chromatin, tubulin, and myosin II. In brains from gio^{RM1}/*Df(3R)D1-BX12* larvae, all early and midtelophase NBs (n = 28) exhibited regular central spindles and myosin rings (data not shown). However, about one half of mutant NBs in late telophase (48%; n = 35) displayed poorly constricted rings (Figure 2C, part b); in

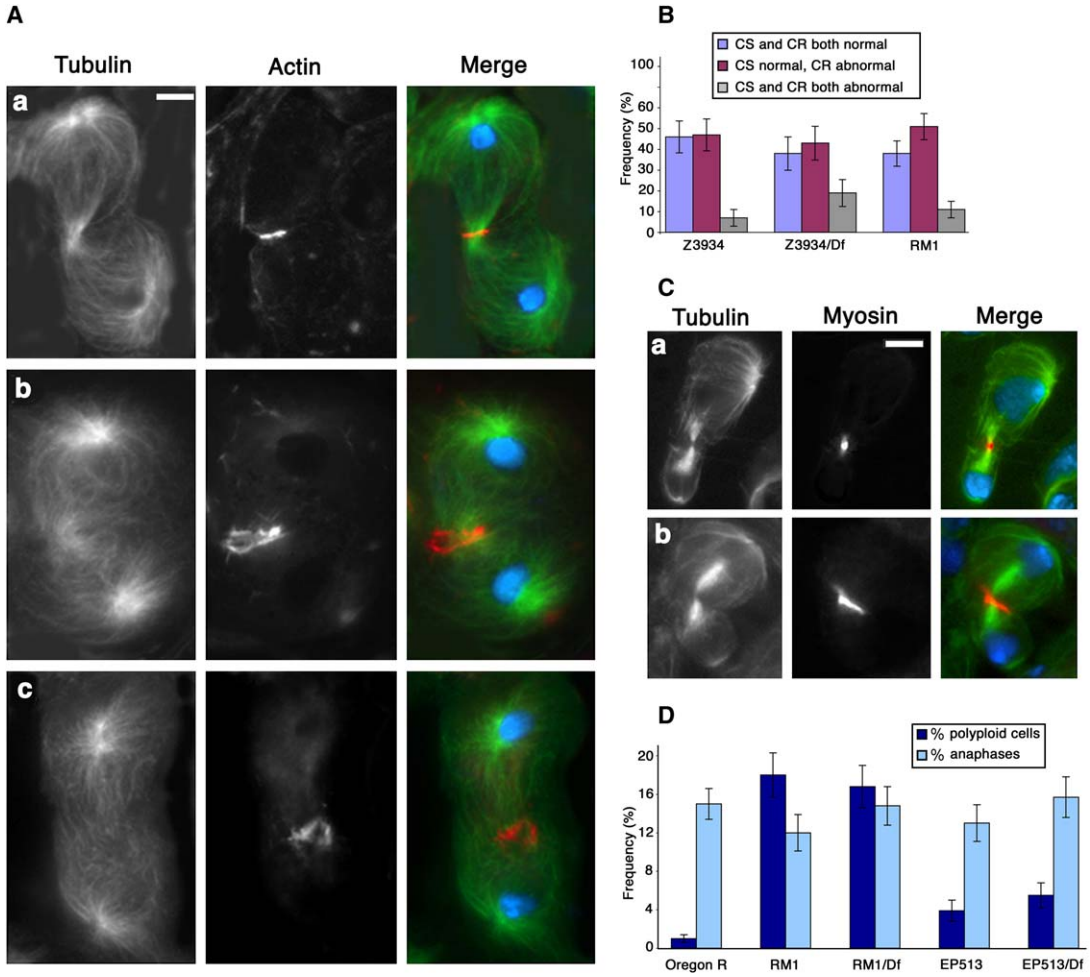

Figure 2. Meiotic and Mitotic Cells from *gio* Mutant Larvae Are Defective in Actomyosin Ring Constriction

(A) Spermatocyte telophases stained for tubulin (green), actin (red), and DNA (blue). (a) Wild-type late telophase; (b) mutant late telophase with an incompletely constricted ring; (c) mutant late telophase with a discontinuous, incompletely constricted ring and a defective central spindle. Scale bar equals 5 μm.

(B) Frequencies (± SE) of irregular late telophases in gio^{Z3934}/gio^{Z3934}, $gio^{Z3934}/Df(3R)D1\text{-}BX12$, and gio^{RM1}/gio^{RM1} mutant males. Defective telophases display incompletely constricted contractile rings (CR) and central spindles (CS) that are either normal or less dense than their wild-type counterparts. In wild-type males, the frequency of irregular CRs and CSs is virtually zero.

(C) Late telophases of wild-type (a) and gio^{RM1}/gio^{RM1} (b) neuroblasts stained for tubulin (green), myosin II (red), and DNA (blue). Note the incompletely constricted actomyosin ring in the mutant telophase. Scale bar equals 5 μm.

(D) Frequencies (± SE) of anaphases and polyploid cells in brains from wild-type (Oregon R), gio^{RM1}/gio^{RM1}, $gio^{RM1}/Df(3R)D1\text{-}BX12$, gio^{EP513}/gio^{EP513}, and $gio^{EP513}/Df(3R)D1\text{-}BX12$ larvae.

wild-type, all NB late telophases (n = 44) consistently showed highly constricted myosin rings (Figure 2C, part a). Collectively, our results indicate that the wild-type function of *gio* is specifically required for actomyosin ring constriction in both mitotic and meiotic cells.

Mutations in *gio* Affect the Distribution of Golgi-Derived Vesicles in Dividing Spermatocytes

Since PITPs have been implicated in budding of secretory vesicles from the trans-Golgi network and in the process of vesicle fusion with the plasma membrane [1], we analyzed the behavior of Golgi-derived vesicles during meiotic division of *gio* mutant males. Vesicles were visualized with antibodies against two different *Drosophila* Golgi proteins: anti-α mannosidase II (GMII) [9] and anti-Lava lamp (Lva) [10]; these antibodies detect identical Golgi structures in germline cells of males [11] (data not shown). In wild-type testes, the Golgi stacks disassemble at metaphase of meiosis I, resulting in numerous vesicle-like structures [11] (data not shown). In most spermatocytes (96%, n = 95) undergoing telophase, these vesicles were concentrated near the poles and excluded from the central region of the cell (Figure 3A, parts a and b). In contrast, 61.7% of *gio* mutant telophases (n = 84) displayed an abnormal localization of vesicle-like structures at the cell equator (Figure 3A, parts c and d). This vesicle phenotype could either be a specific consequence of *gio* mutations or a general consequence of failures in cytokinesis. To discriminate between these possibilities, we examined meiotic division in males hemizygous for the *pebble* male sterile allele pbl^{Z4836} [3]. *pbl* encodes a Rho GEF required for both central spindle assembly and contractile ring formation during both mitotic and meiotic

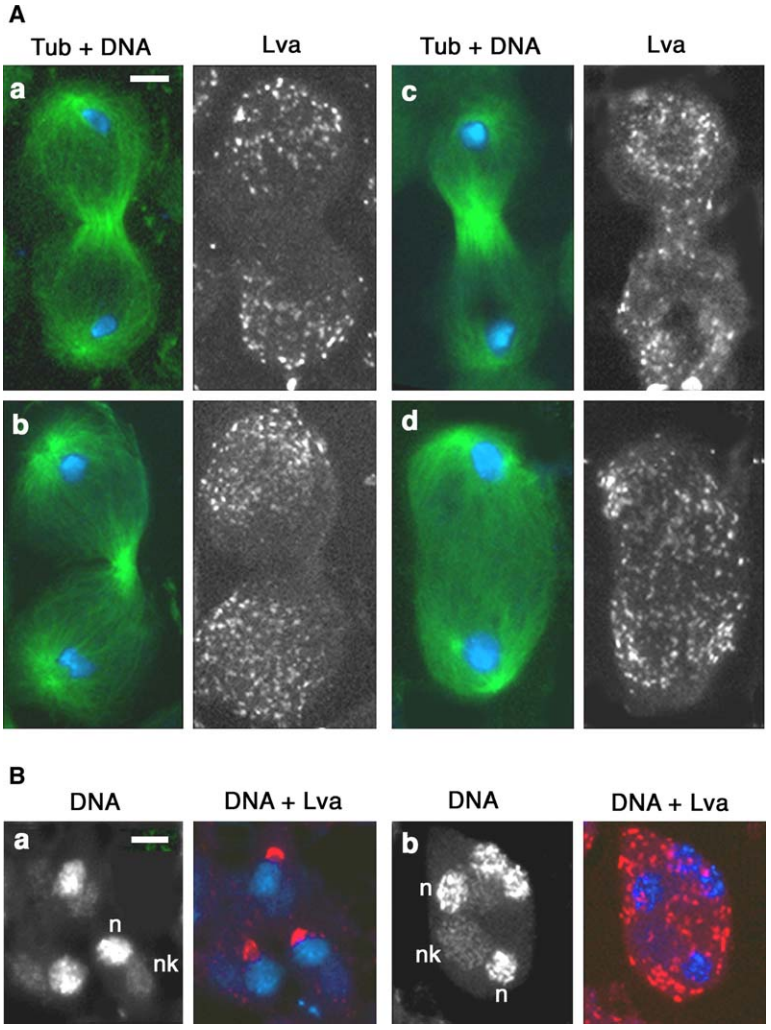

Figure 3. Mutations in *gio* Cause an Abnormal Localization of Golgi-Derived Vesicles during Spermatocyte Division and Affect Acroblast Formation

(A) Visualization of Golgi-derived vesicles in dividing primary spermatocytes by Lva immunostaining. Cells were stained for Lva (black and white panels), tubulin (green), and DNA (blue). In wild-type mid- (a) and late (b) telophases, Golgi vesicles are excluded from the equatorial regions of the cells. In gio^{EP513} mutants, Golgi vesicles display an abnormal localization at the cell equator both in midtelophases with a normal central spindle (c) and in late telophases with a disorganized central spindle (d). Scale bar equals 5 μm.

(B) Wild-type (a) and gio^{EP513} (b) onion stage spermatids stained for Lva (red) and DNA (blue); n, nuclei; nk, nebenkern. Note that the nuclei of wild-type spermatids are associated with Lva-enriched acroblasts; mutant spermatids are associated with many Golgi vesicles but lack organized acroblasts. Scale bar equals 10 μm.

cytokinesis [3, 12]. Immunostaining for Lva of testes from pbl^{Z4836}/*Df(3R)pbl-NR* mutant flies revealed that in 96% of telophases (n = 47), the Golgi-derived vesicles were excluded from the equatorial region of the cell (Figure S2A). These results strongly suggest that the vesicle phenotype observed in *gio* telophases is the cause and not the effect of cytokinesis failures. The most straightforward interpretation of the *gio* phenotype is that the Golgi-derived vesicles fail to fuse with the invaginating furrow membrane, resulting in an abnormal accumulation of these structures at the center of the cell.

These findings prompted us to examine the vesicle phenotype in two additional *Drosophila* cytokinesis mutants implicated in membrane trafficking, *four wheel drive (fwd)* and *four way stop (fws),* which encode a PtdIns 4-kinase and the Cog5 subunit of the conserved oligomeric Golgi complex, respectively [11, 13]. Spermatocytes of both mutants form regular central spindles and contractile rings but are specifically defective in actomyosin ring constriction, just as are *gio* mutant spermatocytes [3, 11, 13]. Analysis of mutant spermatocytes from fwd^{Z0453}/*Df(3L)7C* flies revealed that they exhibit an equatorial localization of Golgi vesicles in 44% of the telophases (n = 61; Figure S2B). In *fws* mutants, vesicle distribution was comparable to wild-type, as only 10% (n = 67) of mutant telophases displayed vesicles at the cell equator (Figure S2C).

Gio Is Required for Acroblast Assembly

In wild-type spermatids, Lva and GMII localize to the acroblast, a structure that forms at the end of the second meiotic division through the aggregation and fusion of Golgi vesicles [4, 11, 14] (Figure 3B, part a; Figure S3A). Wild-type acroblasts are also enriched in the Cog5 protein [11] (Figure S3B) and are stained by fluorescein-conjugated wheat germ agglutinin (WGA); WGA is known to associate with membrane-enriched structures, including the acroblast [15, 16] (Figure S3C). In spermatids from *gio* mutants, Lva, Cog5, and WGA are associated with multiple vesicle-like structures dispersed in the cytoplasm (Figure 3B, part b; Figures S3A–S3C). This suggests that in a *gio* mutant background, the Golgi-derived vesicles fail to fuse with the anterior side of spermatid nuclei, thus preventing acroblast formation. Failures in acroblast assembly due to defective Golgi vesicles fusion have been previously observed in *Drosophila fws* mutants [11] (Figure S2C), as well as in mice lacking the Golgi-associated protein GOPC [17].

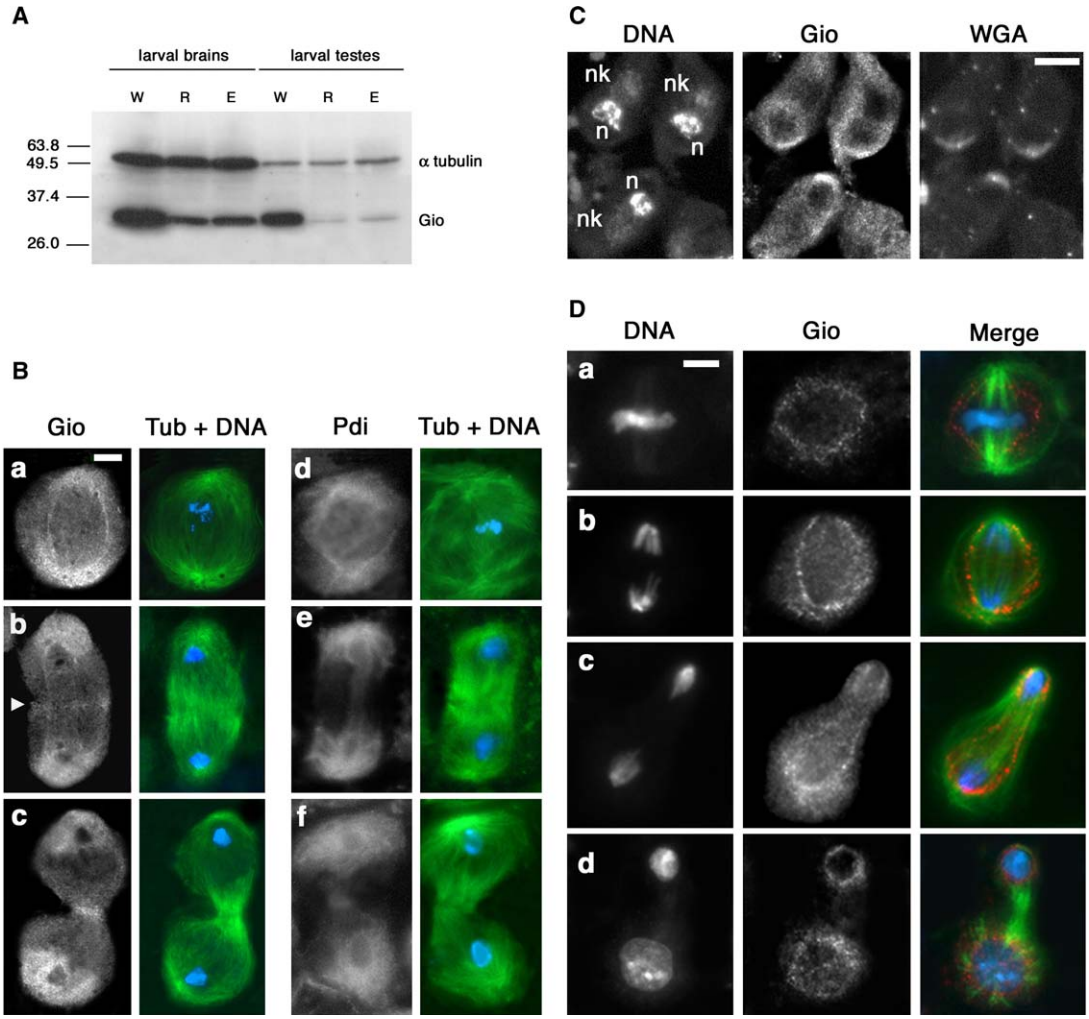

Figure 4. Subcellular Localization of Gio in Spermatocytes, Spermatids, and Larval Neuroblasts

(A) Western blot from brain and testis extracts of wild-type (W), *gio*^{RM1} (R), and *gio*^{EP513} (E) larvae, showing that the anti-Gio antibody recognizes a single band of approximately 35 kDa that is reduced in the mutant tissues. α tubulin was used as loading control.

(B) Gio and Pdi localization in primary spermatocytes. Metaphase (a), early telophase (b), and late telophase (c) figures stained for Gio, tubulin (green), and DNA (blue). Gio is enriched at the cell poles, the spindle envelope, and the cleavage furrow area. Note that Gio starts to concentrate at the cleavage furrow during late anaphase/early telophases (arrowhead in [b]). Metaphase (d), early telophase (e), and late telophase (f) figures from primary spermatocytes expressing GFP-Pdi. Note that Pdi localization largely parallels that of Gio. Scale bar equals 5 μm.

(C) Gio localization in wild-type spermatids. Gio colocalizes with WGA at the anterior side of spermatid nuclei; n, nuclei; nk, nebenkern. Scale bar equals 10 μm.

(D) Gio localization in metaphase (a), anaphase (b), midtelophase (c), and late telophase (d) figures of wild-type larval neuroblasts. Cells were stained for Gio (red), tubulin (green), and DNA (blue). Note that Gio is enriched at the nuclear envelope and at the putative spindle envelope. Scale bar equals 5 μm.

Subcellular Location of Gio

To determine the subcellular localization of Gio, we generated a rabbit polyclonal antibody against the entire protein. Western blotting analysis showed that this antibody recognizes a single polypeptide of ~35 kDa, consistent with the molecular weight of the predicted Gio protein. The amount of this protein was substantially reduced in both brain and testis extracts from *gio* mutant larvae, demonstrating that the antibody specifically reacts with Gio (Figure 4A). Gio was also reduced in the testes of the EMS-induced *gio*^{Z3934} mutant (Figure S4).

Immunostaining of wild-type primary spermatocytes revealed that during metaphase and anatelophase I, Gio accumulates both at the cell poles and at an elliptical structure that encircles the chromosomes (Figure 4B, parts a and b). As spermatocytes progress to telophase, the Gio protein is still visible at the cell poles, but it becomes also enriched at the cleavage furrow area (Figure 4B, parts b and c). The localization of the Gio-enriched structures in meiotic cells is highly reminiscent of the distribution of the endoplasmic reticulum (ER) described by Tates [4, 14]. According to Tates' ultrastructural analysis of dividing spermatocytes, ER consists of parafusorial membranes surrounding the nucleus and astral membranes at the cell poles. Parafusorial membranes have been observed in many invertebrates and are also called "spindle envelope" [18]. Consistent with Gio localization to the ER, the spermatocyte

structures stained by the anti-Gio antibody are largely coincident with those that express the ER marker Protein disulfide isomerase (Pdi) fused with GFP (Figure 4B, parts d–f) [19]. However, there are some interesting differences between Gio and Pdi localization. While Gio concentrates at the cell equator during early telophase (Figure 4B, part b), Pdi does not accumulate in this area until late telophase (Figure 4B, parts e and f). Moreover, while the Gio signal extends across the entire equatorial region of late telophases (Figure 4B, part c), the Pdi signal is limited to the inner part of this region (Figure 4B, part f). These observations suggest that Gio is enriched at the equatorial plasma membrane and that Pdi concentrates within the lumen of the midbody. Consistent with the interpretation that Gio is enriched at cleavage furrow membrane, we have found that Gio colocalizes with the plasma membrane marker FM1-43FX [20] during telophase (Figure S5).

Gio localization in *fws* or *fwd* mutant spermatocytes was comparable to wild-type (data not shown). In spermatocytes of gio^{EP513} mutants, Gio was undetectable (data not shown), further confirming the specificity of our antibody. gio^{EP513} mutants also displayed a normal localization of Pdi (Figure S6), indicating that mutations in *gio* do not induce gross morphological modifications of the ER.

In spermatids, Gio has a rather diffuse cytoplasmic localization and is enriched at the anterior side of nuclei. This nuclear side is also stained by fluorescein-conjugated WGA (Figure 4C), suggesting that Gio accumulates in the area of acroblast assembly.

Immunostaining of wild-type larval brains showed that Gio is mainly cytoplasmic during NB prophase. In subsequent stages of NB mitosis, Gio becomes enriched at the spindle envelope and marks this structure until midtelophase; in late NB telophases, the spindle envelope disappears and Gio concentrates around the reforming nuclei (Figure 4D; the presence of a spindle envelope during NB mitosis has been observed by A.T.C. Carpenter, personal communication). Although Gio localizes to the spindle envelope of both NBs and spermatocytes, we have not been able to detect a clear Gio enrichment at the cleavage furrow area of NB telophases. This observation could reflect either a lower Gio concentration in NBs compared to spermatocytes (see Figure 4A) or the difference in actomyosin ring morphology between these two cell types. NBs form wide actomyosin rings that progressively narrow as cells progress through telophase, while spermatocytes display very narrow actomyosin rings throughout cytokinesis (Figure S7) [3, 21]. If Gio localized to the actin ring-associated membrane, its concentration at the cell equator would be higher in spermatocytes than in NBs.

The Role of Gio in *Drosophila* Cytokinesis

In the past few years, many proteins involved in membrane trafficking have been implicated in animal cell cytokinesis [22]. Our results provide the first demonstration that a class I PITP is required for this process. The other PITP that has been shown to be required for cytokinesis is mammalian Nir2, a class II PITP homologous to *Drosophila* RdgB [2, 7]. However, Gio and Nir2 are likely to play different roles during cytokinesis, as they exhibit different subcellular localizations. While Gio localizes to the ER, Nir2 is primarily enriched at the Golgi structures [2, 7].

Our observations on Gio localization and vesicle behavior in *gio* and *fwd* mutants suggest a model for the role of Gio during *Drosophila* cytokinesis. We propose that Gio mediates transfer of PtdIns monomers to the equatorial membrane of anatelophase cells, thereby causing a local enrichment in PtdIns molecules. An elevated concentration of these lipid monomers and their phosphorylation by the PtdIns 4-kinase encoded by *fwd* would facilitate membrane-vesicle fusion, allowing formation of new membrane and/or vesicle-mediated targeted delivery of proteins required for cytokinesis. However, proper cytokinetic function of the equatorial membrane is likely to require further phosphorylation of PtdIns(4)P molecules, leading to the formation of PtdIns 4,5-biphosphate [PtdIns(4,5)P]. PtdIns(4,5)P has been implicated in cytokinesis in a variety of systems, including *Drosophila* and mammalian cells [23–27].

Although *gio*, *fwd*, and *fws* mutants display different vesicle phenotypes, they have a common cytokinetic defect: they form a normal actomyosin ring, but this ring fails to constrict to completion. These findings indicate that proper membrane trafficking is essential for actin remodeling during animal cell cytokinesis. This conclusion is fully consistent with previous studies carried out both in *Drosophila* and in other organisms. In cellularizing *Drosophila* embryos mutant for syntaxin1, a protein involved in vesicle fusion, the furrow canals lack an organized actin cytoskeleton [28]. Similarly, S2 cells depleted of syntaxin1 by RNAi fail to form actin-based cytokinetic rings [29]. Furthermore, *Dyctyostelium* mutants that lack the vesicle-coating protein clathrin fail to assemble a robust actin ring [30]. Finally, recent studies on crane fly, *Drosophila*, and mammalian cells indicate that PtdIns(4,5)P2 plays an important role in actin ring formation and stabilization [25–27]. Collectively, these results indicate that successful cytokinesis of animal cells requires interactions between the plasma membrane and the actin ring. However, most of the molecules involved in these interactions and their precise biological functions remain to be identified.

Supplemental Data

Supplemental Data include seven figures and Supplemental Experimental Procedures and can be found with this article online at http://www.current-biology.com/cgi/content/full/16/2/195/DC1/.

Acknowledgments

We thank Adelaide T.C. Carpenter for providing us with her unpublished EM images showing the presence of a spindle envelope in dividing *Drosophila* neuroblasts. We are grateful to Hans Buenemann for allowing R.K. to perform some the work described here in his laboratory. We also thank C. Field, D. Roberts, and J. Sisson for the anti-myosin II, anti-α mannosidase, and anti-Lava Lamp antibodies. This work was supported in part by grants from FIRB (RBNE01KXC9-004) and Centro di Eccellenza di Biologia e Medicina Molecolare (BEMM) to M.G. and by the NIH grant IRD-IGM6276 to M.T.F.

Received: August 21, 2005
Revised: November 3, 2005
Accepted: December 2, 2005
Published: January 23, 2006

References

1. Allen-Baume, V., Segui, B., and Cockcroft, S. (2002). Current thoughts on the phosphatidylinositol transfer protein family. FEBS Lett. *531*, 74–80.
2. Lev, S. (2004). The role of the Nir/RdgB protein family in membrane trafficking and cytoskeleton remodeling. Exp. Cell Res. *297*, 1–10.
3. Giansanti, M.G., Farkas, R.M., Bonaccorsi, S., Lindsley, D.L., Wakimoto, B.T., Fuller, M.T., and Gatti, M. (2004). Genetic dissection of meiotic cytokinesis in *Drosophila* males. Mol. Biol. Cell *15*, 2509–2522.
4. Fuller, M.T. (1993). Spermatogenesis. In The Development of *Drosophila melanogaster*, M. Bate and A. Martinez-Arias, eds. (Cold Spring Harbor, NY: Cold Spring Harbor Press), pp. 71–147.
5. Gatti, M., and Baker, B.S. (1989). Genes controlling essential cell cycle functions in *Drosophila melanogaster*. Genes Dev. *3*, 438–453.
6. Rorth, P. (1996). A modular misexpression screen in *Drosophila* detecting tissue-specific phenotypes. Proc. Natl. Acad. Sci. USA *93*, 12418–12422.
7. Litvak, V., Donguha, T., Shari, C., and Lev, S. (2002). Nir2, a human homolog of *Drosophila melanogaster* retinal degeneration B protein, is essential for cytokinesis. Mol. Cell. Biol. *22*, 5064–5075.
8. Hamilton, B.A., Smith, D.J., Mueller, K.L., Kerrebrock, A.W., Bronson, R.T., van Berkel, V., Daly, M.J., Kruglyak, L., Reeve, M.P., Nemhauser, J.L., et al. (1997). The *vibrator* mutation causes neurodegeneration via reduced expression of PITP alpha: positional complementation cloning and extragenic suppression. Neuron *18*, 711–722.
9. Rabouille, C., Kuntz, D.A., Lockyer, A., Watson, R., Signorelli, T., Rose, D.R., van den Heuvel, M., and Roberts, D.B. (1999). The *Drosophila* GMII gene encodes a Golgi alpha-mannosidase II. J. Cell Sci. *112*, 3319–3330.
10. Sisson, J.C., Field, C., Ventura, R., Royou, A., and Sullivan, W. (2000). Lava lamp, a novel peripheral Golgi protein, is required for *Drosophila melanogaster* cellularization. J. Cell Biol. *151*, 905–918.
11. Farkas, R.M., Giansanti, M.G., Gatti, M., and Fuller, M.T. (2003). The *Drosophila* Cog5 homologue is required for cytokinesis, cell elongation, and assembly of specialized Golgi architecture during spermatogenesis. Mol. Biol. Cell *14*, 190–200.
12. Prokopenko, S.N., Brumby, A., O'Keefe, L., Prior, L., He, Y., Saint, R., and Bellen, H.J. (1999). A putative exchange factor for Rho1 GTPase is required for initiation of cytokinesis in *Drosophila*. Genes Dev. *13*, 2301–2314.
13. Brill, J.A., Hime, G.R., Scharer-Schuksz, M., and Fuller, M.T. (2000). A phospholipid kinase regulates actin organization and intercellular bridge formation during germline cytokinesis. Development *127*, 3855–3864.
14. Tates, A.D. (1971). Cytodifferentiation during spermatogenesis in *Drosophila melanogaster*: an electron microscope study. PhD thesis, Rijksuniversiteit de Leiden, Leiden, Netherlands.
15. Lecuit, T., and Wieschaus, E. (2000). Polarized insertion of new membrane from a cytoplasmic reservoir during cleavage of the *Drosophila* embryo. J. Cell Biol. *150*, 849–860.
16. Perotti, M.E., and Pasini, M.E. (1995). Glycoconjugates of the surface of the spermatozoa of *Drosophila melanogaster*: a qualitative and quantitative study. J. Exp. Zool. *272*, 311–318.
17. Yao, R., Ito, C., Natsume, Y., Sugitani, Y., Yamanaka, H., Kuretake, S., Yanagida, K., Sato, A., Toshimori, K., and Noda, T. (2002). Lack of acrosome formation in mice lacking a Golgi protein, GOPC. Proc. Natl. Acad. Sci. USA *99*, 11211–11216.
18. Wolf, K.W. (1995). Spindle membranes and spindle architecture in invertebrates. Micron *26*, 69–98.
19. Bobinnec, Y., Marcaillou, C., Morin, X., and Debec, A. (2003). Dynamics of the endoplasmic reticulum during early development of *Drosophila melanogaster*. Cell Motil. Cytoskeleton *54*, 217–225.
20. Brumback, A.C., Lieber, J.L., Angleson, J.K., and Betz, W.J. (2004). Using FM1–43 to study neuropeptide granule dynamics and exocytosis. Methods *4*, 287–294.
21. Giansanti, M.G., Bonaccorsi, S., and Gatti, M. (2001). The role of centrosomes and astral microtubules during asymmetric division of *Drosophila* neuroblasts. Development *128*, 1137–1145.
22. Albertson, R., Riggs, B., and Sullivan, W. (2005). Membrane traffic: a driving force in cytokinesis. Trends Cell Biol. *15*, 92–101.
23. Matsui, T., Yonemura, S., Tsukita, S., and Tsukita, S. (1999). Activation of ERM proteins in vivo by Rho involves phosphatidyl-inositol 4-phosphate 5-kinase and not ROCK kinases. Curr. Biol. *9*, 1259–1262.
24. Zhang, Y., Sugiura, R., Lu, Y., Asami, M., Maeda, T., Itoh, T., Takenawa, T., Shontoh, H., and Kuno, T. (2000). Phosphatydilinositol 4-phosphate 5-kinase Its3 and calcineurin Ppb1 coordinately regulate cytokinesis in fission yeast. J. Biol. Chem. *275*, 35600–35606.
25. Saul, D., Fabian, L., Forer, A., and Brill, J.A. (2004). Continuous phosphatidylinositol metabolism is required for cleavage of crane fly spermatocytes. J. Cell Sci. *117*, 3887–3896.
26. Field, S.J., Madson, N., Kerr, M.L., Galbraith, K.A.A., Kennedy, C.E., Tahiliani, M., Wilkins, A., and Cantley, L.C. (2005). PtdIns(4,5)P2 functions at the cleavage furrow during cytokinesis. Curr. Biol. *15*, 1407–1412.
27. Wong, R., Hadjiyanni, I., Wei, H.-C., Polevoy, G., McBride, R., Sem, K.-P., and Brill, J.A. (2005). PIP2 hydrolysis and calcium release are required for cytokinesis in *Drosophila* spermatocytes. Curr. Biol. *15*, 1401–1406.
28. Burgess, R.W., Deitcher, D.L., and Schwarz, T.L. (1997). The synaptic protein syntaxin1 is required for cellularization of *Drosophila* embryos. J. Cell Biol. *138*, 861–875.
29. Somma, M.P., Fasulo, B., Cenci, G., Cundari, E., and Gatti, M. (2002). Molecular dissection of cytokinesis by RNA interference in *Drosophila* cultured cells. Mol. Biol. Cell *13*, 2448–2460.
30. Niswonger, M.L., and O'Halloran, T.J. (1997). A novel role for clathrin in cytokinesis. Proc. Natl. Acad. Sci. USA *94*, 8575–8578.